On the Rate Constant for the Association Reaction H + CN + Ar → HCN + Ar

S. P. J. Rodrigues and A. J. C. Varandas*

Departamento de Química, Universidade de Coimbra, P-3049 Coimbra, Portugal

Received: February 17, 1999; In Final Form: May 14, 1999

The importance of the chaperon mechanism (via ArCN or ArH complex formation) is investigated for the title reaction. All calculations employ the classical trajectory method to obtain the reactive cross sections while the equilibrium constants are estimated from statistical mechanics. A detailed analysis of the various approximations to the equilibrium constant is presented. Exploratory calculations based on the energy transfer mechanism are also reported. In addition, the decay rates of the HCN* and ArCN* species are examined in order to get insight on the detailed microscopic molecular dynamics. The chaperon mechanism is found to be important only at low temperatures, while the energy-transfer mechanism dominates for moderate and high ones.

1. Introduction

A termolecular association reaction is traditionally accepted to occur through a sequence of bimolecular collisions involving the formation of metastable quasibound complexes. According to the energy transfer (ET) mechanism,[1−3] the following elementary steps are considered

$$H + CN \rightleftharpoons HCN^* \quad (1)$$

$$Ar + HCN^* \rightarrow Ar + HCN \quad (2)$$

while in the chaperon mechanism (also called radical−molecule or exchange mechanism)[4,5] one has

$$Ar + CN \rightleftharpoons Ar\cdots CN \quad (3)$$

$$H + Ar\cdots CN \rightarrow HCN + Ar \quad (4)$$

$$Ar + H \rightleftharpoons Ar\cdots H \quad (5)$$

$$Ar\cdots H + CN \rightarrow HCN + Ar \quad (6)$$

$$Ar\cdots H + Ar\cdots CN \rightarrow HCN + 2Ar \quad (7)$$

where the dots emphasize the weak nature of the van der Waals bond; these will be omitted henceforword for clarity. Collisions involving larger dimensional clusters of atoms and molecules may also be included in the chaperon mechanism if the study of high pressures is intended,[6] but in the present work we focus on the low-pressure limit. It should be noted that equilibrium (3) is actually a sequence of two equilibria,[5,7] namely

$$Ar + CN \rightleftharpoons ArCN^* \quad (3a)$$

$$ArCN^{\bullet} + Ar \rightleftharpoons ArCN + Ar \quad (3b)$$

with corresponding considerations applying to equilibrium (5). There is also some evidence which indicates that direct three-body collisions may become relevant.[8−10] In addition, we note that there is not a clear cut distinction between the ET and chaperon mechanisms. Indeed, the latter can be understood[11] within a theoretical framework which parallels the resonance theory of Roberts et al.[12] for the ET mechanism. Note that the chaperon and ET mechanisms compete among themselves, their relative importance depending on the nature of the system and reaction conditions, namely temperature and pressure. Indeed, although the ET mechanism has been considered dominant for polyatomic recombination reactions[7,13,14] (see also ref 15 for a review), some early calculations[16] and recent work using the chaperon mechanism[17,18] have led to good agreement with the experimental results.

The main motivation to carry out the present study has been to investigate some of the assumptions in the chaperon mechanism for the title system with special emphasis on the branch involving the ArCN van der Waals molecule. Following previous work,[17,18] this has been done using the classical trajectory method to calculate the rate coefficients, while statistical mechanics has been employed to obtain the equilibrium constants. However, we have also examined another branch of the chaperon mechanism [reactions (5) and (6)] and applied the ET scheme in some exploratory calculations of the title reaction. For this we have used a classical approach similar to that utilized by Blint[19] and Gross and Billing,[20,22] who have followed earlier work by Bunker.[23] Note that a more detailed study taking into account nonequilibrium effects[24] would require the knowledge of the resonance states of HCN*, but these are unavailable and expected to be rather numerous. Finally, we refer to the work of Pack and coworkers[8−10] that suggests that some of the calculations reported in the literature effectively include direct-type three-body collisions. Indeed, if the lifetimes of the complexes are smaller (or on the same order of magnitude) than the time elapsed during the collision with the third body, then the process may be considered three-body like.[9] Of course, a single trajectory has no physical reality in quantum mechanics and hence one should look instead to the average lifetime of the complexes within a bunch of trajectories. Such an analysis is carried out below for the HCN* and ArCN* complexes. All dynamics calculations reported in this work employ the six-dimensional DMBE potential energy surface for the ArHCN van der Waals molecule which has been used elsewhere[25] to study the inverse reaction. Although a novel energy switching (ES) potential surface which shows accurate spectroscopic attributes for ArHCN has meanwhile been reported,[26] it has also been shown[26] that both the DMBE and ES

10.1021/jp9906076 CCC: $18.00
Published on Web 07/23/1999

potential energy surfaces yield similar dynamical attributes for the range of energies (temperatures) considered in the present work.

The plan of the paper is as follows. Section 2 presents the calculations referring to the chaperon mechanism via ArCN formation. A detailed analysis of the required statistical mechanical methods used to calculate the equilibrium constant will be presented in section 2.1. Section 2.2 gives the details of the classical trajectory calculations for the H + ArCN bimolecular reaction and the final chaperon rate constant which has been obtained from various approximations to the equilibrium constant. The chaperon mechanism involving ArH formation is analyzed in section 3, while the calculations on the ET mechanism are presented in section 4. In turn, the detailed analysis of the decay rates for the HCN* and ArCN* complexes is carried out in section 5. Section 6 presents a general discussion and gathers the major conclusions.

2. Chaperon Mechanism via ArCN Formation

Assuming pre-equilibrium, the overall rate constant for reactions (3) and (4) assumes the form

$$k_{\mathrm{chap,l}}(T) = K_{\mathrm{ArCN}}(T) k_{\mathrm{H+ArCN}}(T) \tag{8}$$

where $K_{\mathrm{ArCN}}(T)$ is the equilibrium constant for reaction (3) and $k_{\mathrm{H+ArCN}}(T)$ is a bimolecular rate constant which is calculated here using the classical trajectory technique. As a further assumption, equilibrium constants will be calculated by considering only the molecular bound states. In other words, no reactivity is assumed to occur from the quasibound resonant states of the complexes ArCN. This seems to be a reasonable approximation since a contribution of less than 20% has been observed[27] for diatomic van der Waals systems. This is also corroborated from preliminary calculations of the quasibound states of ArCN*, which we have carried out by assuming a rigid CN bond.

2.1. Equilibrium Constant for ArCN Formation. The equilibrium constant for the reaction Ar + CN ⇌ ArCN can be obtained from statistical mechanics as

$$K(T) = \frac{Q_{\mathrm{tr,ArCN}} Q_{\mathrm{vr,ArCN}}}{Q_{\mathrm{tr,Ar}} Q_{\mathrm{tr,CN}} Q_{\mathrm{vr,CN}}} \exp(-\Delta E_0 / k_{\mathrm{B}} T) \tag{9}$$

where the partition functions for the translational (tr) and vibrational−rotational (vr) degrees of freedom are denoted in the usual way, and ΔE_0 is the energy difference between the equilibrium structures of CN and ArCN.

The "exact" vibrational−rotational partition functions for CN and ArCN can be obtained by counting the states which are obtained from a rigorous solution of the nuclear Schrödinger equation. Yet, since CN is a bound molecule with a deep well, the harmonic oscillator (HO) plus rigid rotator (RR) models can provide a good approximation for the calculation of its vibrational−rotational partition function at the sampled temperatures. In fact, as will be shown later, an improved test calculation of the partition function for this molecule (which has been carried out using an anharmonic vibrotor model) led to results essentially identical to those obtained from the simple HO+RR model, except for at high temperatures. However, such conditions no longer hold for the case of ArCN, which is known to be a weakly bound and very floppy molecule. As a result, most vibrational−rotational states will be occupied even for low temperatures, with the vibrational−rotational partition function being proportional to the (finite) number of such vibrational−rotational states when $k_{\mathrm{B}}T \gg D_{\mathrm{e}}$.[28] Since the strong vibration of CN is essentially decoupled from the remaining modes of the ArCN van der Waals molecule, it would seem a good approximation to calculate its vibrational−rotational levels in the atom−rigid diatomic approximation. In this case the partition function due to the vibrational frequencies of CN in the van der Waals molecule would cancel its equivalent partition function for the "free" CN molecule when calculating the equilibrium constant in eq 9. As shown below, this appears indeed to be a good approximation for the temperatures sampled in the present work.

Using the potential energy surface for the fragment ArCN molecule, all bound vibrational−rotational levels of the two-dimensional (2D) atom−rigid diatom system have been calculated using the BOUND[29,30] computer code. Specifically, the close-coupled equations were set up including all the CN rotor functions up to $j = 10$ (for the cyanogen rotational constant, we have used $B_{\mathrm{e}} = 1.8989\ \mathrm{cm}^{-1}$), and the coupled equations propagated between $R_{\mathrm{min}} = 2.6$ Å and $R_{\mathrm{max}} = 14.0$ Å with a step size of $\mathrm{d}R = 0.05$ Å. With the chosen parameters, a convergence better than $0.05\ \mathrm{cm}^{-1}$ is estimated, which is more than enough for the calculations reported in the present study. The calculations predicted a total of 667 energies, denoted formally as E_{vJ}, with the maximum allowed total angular momentum being found to be $J = 27$. Using this data, the "exact" 2D vibrational−rotational partition function $Q_{\mathrm{vr}}^{\mathrm{E2D}}$ of the ArCN molecule can be estimated through the sum

$$Q_{\mathrm{vr}}^{\mathrm{E2D}} = \sum_{\mathrm{vJ}} (2J+1) \exp\left(-\frac{E_{\mathrm{vJ}}}{k_{\mathrm{B}}T}\right) \tag{10}$$

Note that some approximations to this sum have been used in the past.[17] In all of them the atom−diatom vibrational motion has been separated from rotation, which may lead to problems for a floppy van der Waals molecule such as ArCN, since the two rotational modes (i.e., the hindered and overall rotations) are expected to be coupled to the stretching atom−diatom coordinate. For completeness, we discuss some of these approximations in the following paragraphs.

The simplest approximation to the vibrational partition function is the HO one, according to which one has

$$Q_{\mathrm{v}}^{\mathrm{HO}} = \prod_{i=1}^{3} \frac{\exp(-hc\nu_i / 2k_{\mathrm{B}}T)}{1 - \exp(-hc\nu_i / k_{\mathrm{B}}T)} \tag{11}$$

where υ_{i} are the harmonic frequencies of the van der Waals molecule. Clearly, this is a very crude approximation, not only because the van der Waals modes are highly anharmonic but also because dissociation is not taken into consideration as mentioned above. In turn, the RR approximation leads to

$$Q_{\mathrm{r}}^{\mathrm{RR}} = \left[\pi \left(\frac{8\pi^2 I_A}{h^2}\right)\left(\frac{8\pi^2 I_B}{h^2}\right)\left(\frac{8\pi^2 I_C}{h^2}\right)\right]^{1/2} \tag{12}$$

where I_α ($\alpha = A, B, C$) are the principal inertia moments of the molecule. A free internal rotor (FIR) approximation has also been tested in ref 17. In this model, the vibrational partition function, which is calculated from the "exact" stretching energies

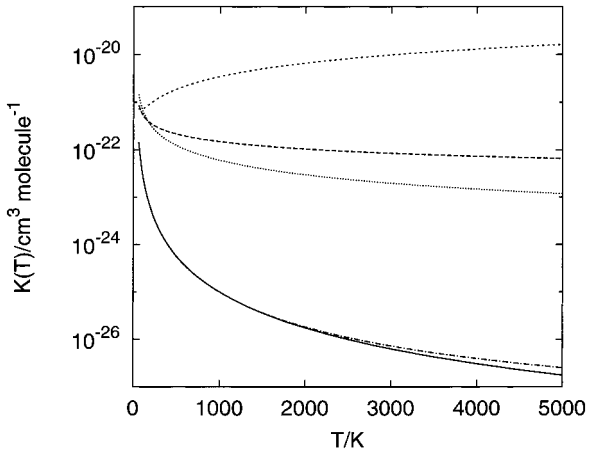

Figure 1. Calculated equilibrium constants for Ar + CN ⇌ ArCN: (-·-) "exact" 2D vibrational−rotational partition function for ArCN with CN treated as a rigid rotor; (—) as in the previous case but with CN treated as a anharmonic vibrating rotor; (---) HO+RR model; (···) "exact" 2D vibrational ($J = 0$) partition function with the RR model; (— — —) "exact" pseudodiatomic vibrational partition function with the FIR model. See the text for details.

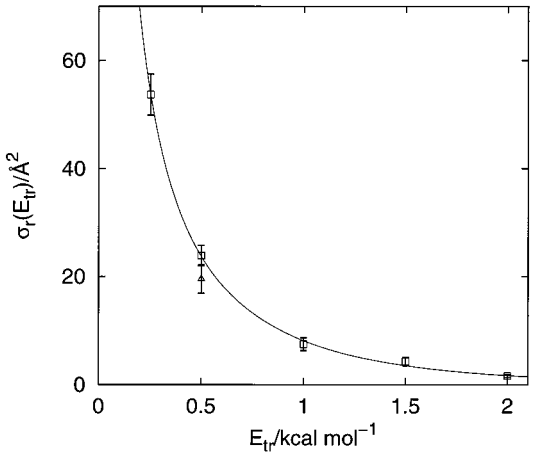

Figure 2. Cross sections for the bimolecular reaction H + ArCN, □ and —; calculation with vibrational energy on the van de Waals modes of ArCN, △.

E_n of the isotropic pseudodiatomic molecule Ar−CN, assumes the form

$$Q_v^{FIR} = \sum_n \exp\left(-\frac{E_n}{k_B T}\right) \tag{13}$$

while the rotation of CN is considered to be free (zero-anisotropy approximation). In addition, the rotational partition functions are assumed to be the classical ones, namely

$$Q_r^{FIR} = \left(\frac{8\pi^2 I_{Ar-CN}}{h^2}\right)\left(\frac{8\pi^2 I_{pd}}{h^2}\right) \tag{14}$$

where I_{Ar-CN} represents the inertial moment of the pseudodiatomic molecule and $I_{pd} = I_{CN}\ (1 - \sum_{\alpha=1}^{3} I_{CN\gamma\alpha}/I_\alpha)$ is the reduced inertial moment of the diatomic molecule; γ_α are the director cosines between the axis of the diatomic and the α principal axis. Finally, another approximate model has been tested. Specifically, the partition function for the van der Waals vibrational modes of the ArCN molecule has been calculated accurately using the corresponding nonrotating values (which are obtained from the 2D calculations referred to above) while the rotation has been estimated within the RR model of eq 12.

Figure 1 shows the equilibrium constants that have been calculated from the various models once the partition functions were replaced in eq 9. As it might have been expected, the HO+RR model is clearly unphysical with the equilibrium constant growing with temperature. Although showing a correct physical decrease with temperature, the other models show differences of various orders of magnitude. Moreover, we observe that the influence of anharmonicity in the vibrational−rotational partition function of CN is small but relevant above 1500 K.

2.2. HCN Formation via H + ArCN. The trajectory calculations have been carried out using a modified version[17,18,25] of the MERCURY program.[31] The optimized time steps have been found to be in the interval $(0.8-1.0) \times 10^{-16}$ s and the trajectories integrated until reaction occurred through one of the reactive channels or the limiting time $(4.8-6.0) \times 10^{-11}$ s (6.0×10^5 time steps of integration) was attained. The maximum impact parameters b_{max} have been estimated by running small batches of trajectories (typically 60) for fixed values of b and their optimum values chosen as the minimum value of b for which no reactivity within the relevant channel was observed. All channels have been identified by employing the procedure reported elsewhere;[17,18,25] for a detailed description of the various reactive channels, the reader is referred to ref 25.

The cross section for the reaction of H with ArCN has been considered to depend only on the relative translational energy, while the internal energy of ArCN was taken to be zero. This approximation is equivalent to assuming that all the internal vibrational rotational states of ArCN have a similar reactivity. To gain some insight on this issue, a few calculations have been carried out with an amount of internal energy on the ArCN molecule below the threshold corresponding to the ArCN dissociation. This has been found to have no significant implications on the final outcomes. Indeed, as shown in Figure 2, the inclusion of 0.1 kcal mol^{-1} of vibrational energy on the van der Waals modes of ArCN seems to have no relevant effect on reactivity. Of course, calculations with larger amounts of vibrational energy on the CN molecule are not feasible, due to energy leakage to the weak van der Waals modes.[17] Indeed, dissociation frequently takes place in this case at some early stage of the collisional process.

To describe the cross section dependence on the translational energy, we have used the following excitation function[32]

$$\sigma_S(E_{tr}) = CE_{tr}^n \exp(-mE_{tr}) \tag{15}$$

where $C = 21.8$ Å^2/(kcal mol^{-1})^n, $m = 0.98$ kcal mol^{-1}, and $n = -0.825$ are adjustable parameters which have been determined from a least-squares fit to the calculated cross sections given in Table 1. The quality of the fit is seen from Figure 2 to be quite good. After integration over the translational energy, eq 15 yields for the analytical rate coefficient

$$k_{H+ArCN}(T) = gC\left(\frac{8k_B T}{\pi\mu_{H+ArCN}}\right)^{1/2} \frac{(k_B T)^n}{(1 + mk_B T)^{n+2}}\Gamma(n+2) \tag{16}$$

where $g = 1/4$ is the electronic degeneracy factor, μ_{H+ArCN} the atom−triatom reduced mass, and Γ the gamma function. The calculated rate constants for the various approximations which have been used in the calculation of the chaperon mechanism via ArCN formation (i.e., for the various approximations used

TABLE 1: Summary of the Trajectory Calculations for the H + ArCN Reaction

E_{tr}/kcal mol^{-1}	b_{max}/Å	N_{tot}	N_{HCN*}[a]	N_{HCN}[a]	σ_{H+ArCN}/Å^2
0.25	8.2	500	156	120	50.7 ± 4.0
0.50	8.0	999[b]	381	123	24.8 ± 2.1
1.0	8.0	1000	391	40	8.0 ± 1.3
1.5	7.6	1000	397	29	4.2 ± 0.9
2.0	7.2	1000	413	10	1.6 ± 0.5

[a] N_{HCN} denotes the number of trajectories leading to formation of stable HCN, while N_{HCN*} represents the corresponding number for formation of unstable HCN*. [b] One trajectory was incomplete after the allowed integration time and was removed from the statistics.

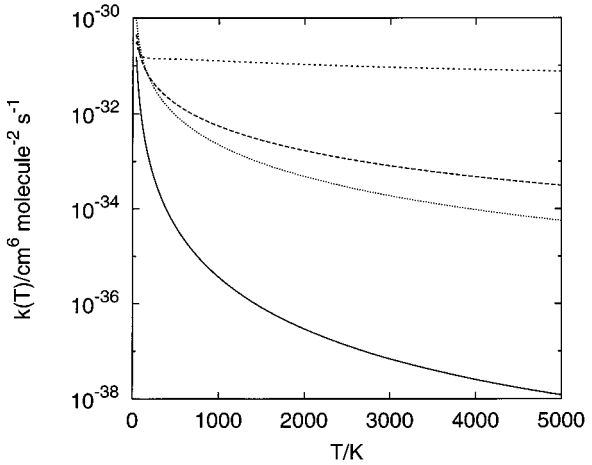

Figure 3. Chaperon rate coefficient for the H + CN + Ar → HCN + Ar association reaction (via H + ArCN): (—) "exact" 2D vibrational-rotational partition function for ArCN with CN treated as a anharmonic vibrating rotor; (---) HO+RR model; (···) "exact" 2D vibrational (J = 0) partition function with RR model; (— — —) "exact" pseudodiatomic vibrational partition function with FIR model. See the text for details.

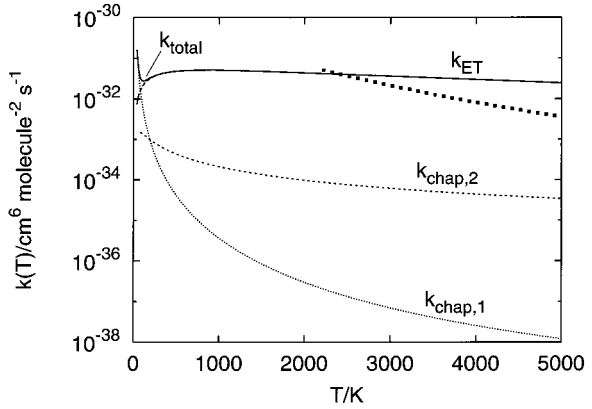

Figure 4. Thermal rate coefficient for the H + CN + Ar → HCN + Ar association reaction: (------) k_{ET}, energy transfer mechanism; (···) $k_{chap,1}$ chaperon mechanism (via H + ArCN); (---) $k_{chap,2}$, chaperon mechanism (via ArH + CN); (—) k_{total}, sum of the rate coefficients of the above mechanisms; ■, experimental (obtained from refs 36 and 37). See the text for details.

to obtain the equilibrium constant in eq 3) are presented in Figure 3. They have been obtained by multiplying the relevant equilibrium constant by the bimolecular rate coefficient, as indicated in eq 8. Clearly, there are notable differences between the various approximations. A comparison with the available experimental data can be found in Figure 4. However, we should qualify at this stage what we mean by experimental data. Indeed, although there are some experimental[33−35] and evaluated[36] data for the inverse dissociation reaction HCN + Ar → H + CN + Ar, the reaction of interest here has, to our knowledge, not been studied experimentally. For the association reaction, Tsang[37] only published estimates of the kinetics coefficients constants for cases where the third-body was N_2 and CO_2 but not Ar. We have taken the values he reports for the equilibrium constant to estimate the experimental data shown in Figure 4. These have been calculated by multiplying the recommended[36] rate constant for the dissociation reaction by the H + CN ⇌ HCN equilibrium constant,[36,37] i.e., $k^{exp}_{rec,0}(T) = k^{exp}_{diss,0}(T)K_c(T)$. Although the agreement with the results from the HO+RR and FIR models seems best, this is perhaps fortuitous and probably due to some cancellation of errors.

TABLE 2: Summary of the Trajectory Calculations for the ArH + CN Reaction

E_{tr}/kcal mol^{-1}	b_{max}/Å	N_{tot}	N_{HCN}[a]	σ_{ArH+CN}/Å^2
0.25	9.0	1000	62	15.8 ± 1.9
0.50	9.0	1000	45	11.4 ± 1.7
1.0	8.8	1000	38	9.2 ± 1.5
1.5	8.7	1000	40	9.5 ± 1.5
2.0	8.6	1000	39	9.1 ± 1.4
4.0	8.3	1000	40	8.7 ± 1.3
8.0	8.2	1000	46	9.7 ± 1.4
16.0	8.2	1000	28	5.9 ± 1.1
24.0	8.2	1000	31	6.6 ± 1.2

[a] N_{HCN} denotes the number of trajectories leading to formation of stable HCN.

3. Chaperon Mechanism via ArH Complex Formation

Assuming pre-equilibrium, the rate constant $k_{chap,2}(T)$ for the chaperon branch involving the reactions (5) and (6) takes the form

$$k_{chap,2}(T) = K_{ArH}(T)k_{ArH+CN}(T) \qquad (17)$$

where $K_{ArH}(T)$ is the equilibrium constant of reaction (5) and $k_{H+ArCN}(T)$ is the associated bimolecular rate constant. The equilibrium constant can in this case be easily estimated from statistical mechanics by using the vibrational−rotational energy levels of ArH, which have been calculated by solving the nuclear Schrödinger equation. This calculation is essentially exact for a given potential energy curve, and hence the calculated equilibrium constant should be very accurate.

Similarly to the other chaperon branch mechanism studied in section 2, the classical trajectory approach has been used to estimate k_{ArH+CN}. The main difference from the preceding calculation concerns the initial conditions of the reactants. In the present case, the trajectories have been initiated with zero point energy on both diatomic molecules. In addition, to be consistent, the outcoming HCN molecules are considered stable only when its internal energy lies below the sum of its classical dissociation energy plus zero-point energy of CN. This is an approximate scheme to include the quantum mechanical threshold energy, which appears adequate for the present purposes. More elaborate treatments of this problem (which, of course, can only be overcome through rigorous quantum/semiclassical calculations) have been discussed in ref 38 and references therein to which the reader is referred for details.

As in the previous case, the classical trajectory studies have been carried out by using a modified version[17,18,25] of the MERCURY program[31] (all technical details are similar to those presented above). The cross sections obtained for this collisional system are shown in Table 2 and have been fitted to eq 15 with $m = 0$. The calculated parameters are $C = 10.71$ Å^2/(kcalmol^{-1})^n and $n = -0.183$. After integration over the translational energy,

TABLE 3: Summary of the trajectory calculations for the study by the ET mechanism[a]

E_{tr}^{3b}/kcal mol^{-1}	N_{HCN^*}	$<t_{HCN^*}>/\pi b_{max,3b}^2/10^{-14}$ s	E_{tr}^{4b}/kcal mol^{-1}	N_{HCN}	σ_{ET}/Å^2
1.0	833	253	0.5	29	3.4 ± 0.6
			1.0	33	3.9 ± 0.7
			4.0	34	4.0 ± 0.7
			8.0	31	3.7 ± 0.6
			12.0	33	3.9 ± 0.7
2.0	749	190	1.0	7	0.9 ± 0.4
			2.0	17	2.2 ± 0.5
			4.0	18	2.4 ± 0.6
			8.0	17	2.2 ± 0.5
			12.0	25	3.3 ± 0.6
			20.0	19	2.5 ± 0.6
4.0	651	107	1.0	2	0.3 ± 0.2
			4.0	9	1.4 ± 0.5
			8.0	9	1.4 ± 0.5
			12.0	13	2.0 ± 0.5
6.0	585	67	4.0	1	0.2 ± 0.2
			8.0	4	0.7 ± 0.3
			12.0	2	0.3 ± 0.2

[a] For all runs, 10^3 trajectories have been used, with b_{max} values being 6.0 Å for the complex formation reaction (N_{HCN^*}) and 5.6 Å for the stabilization process (N_{HCN}).

the analytical rate coefficient assumes the form

$$k_{ArH+CN}(T) = gC\left(\frac{8k_BT}{\pi\mu_{ArH+CN}}\right)^{1/2}(k_BT)^n\Gamma(n+2) \quad (18)$$

where μ_{ArH+CN} is the diatomic−diatomic reduced mass. The calculated rate constant $k_{chap,2}(T)$ is depicted graphically in Figure 4.

4. Energy Transfer Mechanism

Similarly to the work of Gross and Billing,[21] our energy transfer calculations have been carried out in two steps. First, we introduce the notion of HCN* complex as a species in which the bond distances satisfy the relations $R_{CN} < 1.404$ Å, $R_{CH} < 2.556$ Å, and $R_{NH} < 2.676$ Å. The lifetimes of the HCN* complexes are next calculated as a function of the translational energy of the H + CN collisional system (E_{tr}^{3b}). For each trajectory, the time, coordinates, and momenta are then registered at the initial moment of complex formation, with the trajectory being allowed to continue until dissociation. Obviously, the difference between the final and initial times is the complex lifetime. More specifically, the lifetime of a molecular complex is taken as the time interval between the entrance in the predefined configurational volume and the formation of products. One should note at this stage that, for high impact parameters, some of the trajectories do not form a complex and its lifetime is consequently assumed as zero for the Monte Carlo integration. We further note that all calculations have been carried out for the ground vibrational−rotational state of CN, and hence, the present results should be viewed as exploratory.

In a second step, the recorded coordinates and momenta are used to start the collisional process involving HCN* and Ar. This allows us to calculate the cross section dependence on the translational energy of the Ar + HCN* collisional process (E_{tr}^{4b}). Note that this cross section depends on E_{tr}^{3b} and that only HCN molecules with an energy value smaller than the quantum threshold for dissociation have been considered as stable triatomic products. Once more, a specific modified version of the MERCURY program[3l] has been utilized, with most of the technical details being identical to those already described. The maximum impact parameter has been fixed at $b_{max,3b} = 6.0$ Å for the first step and $b_{max,4b} = 5.6$ Å for the second step. As before, these values have been optimized by running batches of trajectories for trial b values. The thermal rate constant for the ET process can then be expressed as

$$k_{ET}(T) = \frac{8k_BT}{\pi(\mu_{3b}\mu_{4b})^{1/2}(k_BT)^4}\int_0^\infty dE_{tr}^{3b}\,E_{tr}^{3b} \times \exp(-E_{tr}^{3b}/k_BT)\langle t_{HCN^*}\rangle \times \int_0^\infty dE_{tr}^{4b}\,E_{tr}^{4b} \times \exp(-E_{tr}^{3b}/k_BT)\sigma_{ET} \quad (19)$$

where

$$\langle t_{HCN^*}\rangle = \int_0^{b_{max}} db\; b t_{HCN^*} \simeq \frac{\sum_{i=1}^N t_{i,HCN^*}}{N}\pi b_{max,3b}^2 \quad (20)$$

is the Monte Carlo integration over the impact parameters of the lifetimes, μ_{3b} is the reduced mass of the H + CN system, and μ_{4b} is the reduced mass of the Ar + HCN system. The calculated lifetimes of the HCN* complexes are presented in Table 3 and can be represented by the exponential form

$$\frac{<t_{HCN^*}>}{\pi b_{max,3b}^2} = T_0\exp(-T_1E_{tr}^{3b}) \quad (21)$$

where $T_0 = 332 \times 10^{-14}$ s and $T_1 = 0.28$ (kcal mol^{-1})$^{-1}$. The calculated cross sections for the stabilization reaction are also shown in Table 3. They can be fitted to the excitation function

$$\sigma_{ET}(E_{tr}^{3b}, E_{tr}^{4b}) = c_0\exp(-c_1E_{tr}^{3b})\,(E_{tr}^{4b} - E_0)/E_{tr}^{4b} \quad E_{tr}^{4b} - E_0 > 0 \quad (22)$$

$$= 0 \qquad E_{tr}^{4b} - E_0 \le 0$$

where $E_0 = d_0(E_{tr}^{3b})^2$. The values of the calculated parameters are $c_0 = 5.35$ Å^2, $c_1 = 0.306$ (kcal mol^{-1})$^{-1}$, and $d_0 = 0.0591$ kcal mol^{-1}. Figure 4 shows the corresponding calculated rate constant $k_{ET}(T)$. A decrease of this rate constant for lower temperatures appears to be typical[11,19−22] for the ET mechanism; the reader is referred to ref 9 and references therein for discussion on this topic. Of course, the calculated rate constant vs temperature dependence may be sensitive to the analytical form employed to represent the excitation function at energies near threshold. This is difficult to determine accurately, since

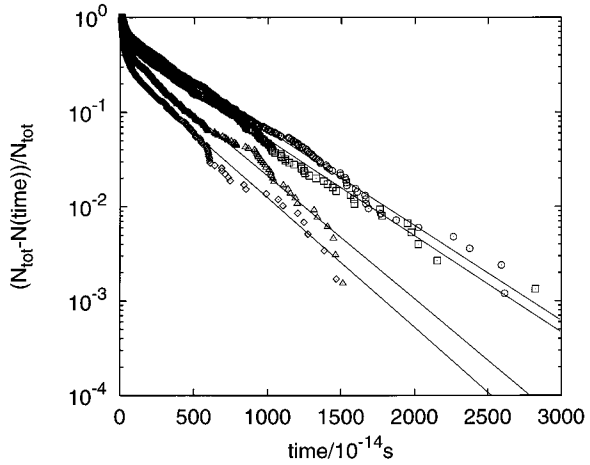

Figure 5. Decay rate for the HCN* molecules as a function of time and translational energy: (○) $E_{tr} = 1.0$ kcal mol^{-1}; (□) $E_{tr} = 2.0$ kcal mol^{-1}; (△) $E_{tr} = 4.0$ kcal mol^{-1}; (◇) $E_{tr} = 6.0$ kcal mol^{-1}. See the text for the fitted curves.

it would require substantially more calculations. Given the approximations involved in preparing the initial states of the CN molecule, we did not judge them to be warranted in the present work. In summary, the main feature of the present results seems to be the overestimation of the experimental results at high temperatures. Although this could be attributed, of course, to inaccuracies of the potential energy surface, we believe that the main cause is the classical approach itself. In fact, the classical method that we employ treats the quasibound states as a continuum and hence leads to an overestimation of the equilibrium constant for metastable HCN* formation.

5. Lifetime of the Complexes HCN* and ArCN*

The lifetimes of HCN* and ArCN can give some insight on the importance of the mechanisms discussed above. Indeed, the results for the ET calculations of the previous section can be used to obtain the decay rates of the HCN* energized molecules, which are presented in Figure 5. As reported in previous work for the HO_2 radical,[18,39] such decays appear to follow a two-step mechanism

$$HCN^* \xrightarrow{k_1} HCN^{\ddagger} \xrightarrow{k_2} H + CN \qquad (23)$$

which can can be fitted to the form[18]

$$f(t) = \left(f^0_{HCN^{\ddagger}} - \frac{k_1 f^0_{HCN^*}}{k_2 - k_1}\right)\exp(-k_2 t) + \left(f^0_{HCN^*} + \frac{k_1 f^0_{HCN^*}}{k_2 - k_1}\right)\exp(-k_1 t) \quad (24)$$

where $f^0_{HCN^*}$, and $f^0_{HCN^{\ddagger}}$ denote the fraction of HCN* and HCN‡ present at $t = 0$; as usual, HCN‡ indicates some intermediate species (bottleneck) for the dissociation process. The values obtained from a least squares fit to this expression are presented in Table 4, while the quality of the fit can be appreciated from Figure 5. As expected, the higher the energy, the greater the amount of promptly dissociating complexes. This is reflected not only by the lowering of the mean lifetime but also by the increase of the effective three-body collisions produced in the second step of the ET method.

Classical trajectory calculations similar to those carried out for the ET mechanism have also been done for the collisional

TABLE 4: Parameters Obtained by Fitting the Decay Rates of HCN• to eq 24

E_{tr}/kcal mol^{-1}	$f^0_{HCN^*}$	$k_1/10^{14}$ s^{-1}	$k_2/10^{14}$ s^{-1}
1.0	0.30	0.0023	0.019
2.0	0.41	0.0024	0.023
4.0	0.51	0.0030	0.027
6.0	0.64	0.0032	0.033

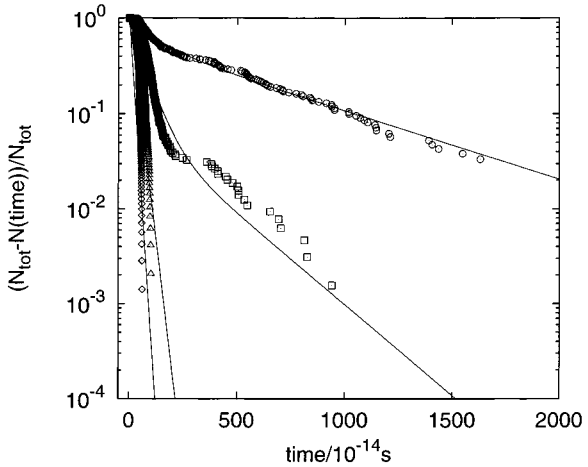

Figure 6. Decay rate for the ArCN* molecules as a function of time and translational energy: (○) $E_{tr} = 0.05$ kcal mol^{-1}; (□) $E_{tr} = 0.25$ kcal mol^{-1}; (△) $E_{tr} = 0.50$ kcal mol^{-1}; (◇) $E_{tr} = 1.0$ kcal mol^{-1}. See the text for the fitted curves.

TABLE 5: Parameters Obtained by Fitting the Decay Rates of ArCN* to eq 24

E_{tr}/kcal mol^{-1}	$f^0_{HCN^*}$	$k_1/10^{14}$ s^{-1}	$k_2/10^{14}$ s^{-1}
0.05	0.33	0.0016	0.0085
0.25	0.68	0.0044	0.017
0.50	1.0		0.043
1.00	1.0		0.076

system Ar + CN. The results for the stability of the ArCN complexes are presented as decay rates in Figure 6 and Table 5. Almost all trajectories with lifetimes less than 10^{-13} s correspond only to the crossing of the particles through the configurational zone of the complex within a period of vibration, as verified by analyzing their time evolution. This is the case for all calculated trajectories with translational energies 0.5 and 1.0 kcal mol^{-1}, for which formation of metastable complexes was not detected. Regarding the translational energies 0.05 and 0.25 kcal mol^{-1}, there are clearly two regimes: one corresponding to formation of long-lived complexes (translational energies above about 0.25 kcal mol^{-1}), and the other corresponding to quasidirect collisions. Thus, from a dynamical point of view, the stabilization of the chaperon ArCN* complexes appears to be statistically significant only for low energies corresponding to temperatures smaller than 200 K or so. This may explain why the chaperon rate constant is very small for high temperatures, as verified in previous sections of this work.

6. Discussion and Conclusions

As pointed out by Pack and co-workers,[9,10] the rate constants for the collision-induced dissociation and association reactions are related by the detailed balance, while their cross sections are related by microscopic reversibility. As a result, both reactions must proceed via the same microscopic mechanism, one being the reverse of the other. Concerning this issue, we have noted in our previous classical trajectory study[25] of the inverse reaction that the most important route for dissociation

is via a two-step mechanism in which a long-lived energized HCN* complex is formed. The direct dissociation reaction through a short-lived complex is less important but increases with temperature. In turn, formation of ArCN + H and ArH + CN is almost negligible. The results of the present work are also consistent with such previous results for the collision-induced dissociation process, as one would expect from microscopic reversibility. Yet, the results calculated in the present work for the chaperon mechanism could not be anticipated from our studies of the inverse reaction, because much lower energies and temperatures are now involved. The investigation carried out in the present work also allows us to conclude that, for the title system (and possibly for similar triatomic ones), the chaperon mechanism is relevant for the low-temperature regime while the ET mechanism is probably dominant for moderate and high temperatures.

Acknowledgment. This work has the support of the Fundação para a Ciência e Tecnologia, Portugal, under programme PRAXIS XXI.

References and Notes

(1) Lindemann, F. A. *Trans. Faraday Soc.* **1922**, *17*, 598.
(2) Hinshelwood, C. N. *Proc. Roy. Soc. A* **1927**, *113*, 230.
(3) Steiner, W. *Z. Physik. Chem.* **1932**, *B15*, 249.
(4) Kimball, G. *E. J. Am. Chem. Soc.* **1932**, *54*, 2396.
(5) Bunker, D. L.; Davidson, *N. J. Am. Chem. Soc.* **1958**, *80*, 5090.
(6) Burns, G.; Wong, W. H. *J. Am. Chem. Soc.* **1975**, *97*, 710.
(7) Porter, G. *Discussions Faraday Soc.* **1962**, *33*, 198.
(8) Pack, R. T; Walker, R. B.; Kendrick, B. K. *Chem. Phys. Lett.* **1997**, *276*, 255.
(9) Pack, R. T; Walker, R. B.; Kendrick, B. K. *J. Chem. Phys.* **1998**, *109*, 6701.
(10) Pack, R. T; Walker, R. B.; Kendrick, B. K. *J. Chem. Phys.* **1998**, *109*, 6714.
(11) Pack, R. T; Snow, R. L.; Smith, W. D. *J. Chem. Phys.* **1971**, *56*, 926.
(12) Roberts, R. E.; Bernstein, R. B.; Curtis, C. F. *J. Chem. Phys.* **1969**, *50*, 5163.
(13) Eusuf, M.; Laidler, K. J. *Trans. Faraday Soc.* **1963**, *59*, 2750.
(14) Whitlock, P. A.; Muckerman, J. T.; Roberts, R. E. *J. Chem. Phys.* **1974**, *60*, 3658.
(15) Troe, J. *Annu. Rev. Phys. Chem.* **1978**, *29*, 223.
(16) Kim, S. K. *J. Chem. Phys.* **1967**, *46*, 123.
(17) Varandas, A. J. C.; Pais, A. A. C. C.; Marques, J. M. C.; Wang, W. *Chem. Phys. Lett.* **1996**, *249*, 264.
(18) Marques, J. M. C.; Wang, W.; Pais, A. A. C. C.; Varandas, A. J. C. *J. Phys. Chem.* **1996**, *100*, 17513.
(19) Blint, R. J. *J. Chem. Phys.* **1980**, *73*, 765.
(20) Gross, A.; Billing, G. D. *Chem. Phys.* **1993**, *173*, 393.
(21) Gross, A.; Billing, G. D. *Chem. Phys.* **1994**, *187*, 329.
(22) Gross, A.; Billing, G. D. *Chem. Phys.* **1997**, *217*, 1.
(23) Bunker, D. L. *J. Chem. Phys.* **1960**, *32*, 1001.
(24) Schwenke, D. W. *J. Chem. Phys.* **1990**, *92*, 7267.
(25) Rodrigues, S. P. J.; Varandas, A. J. C. *J. Phys. Chem.* **1998**, *102*, 6266.
(26) Varandas, A. J. C.; Rodrigues, S. P. J.; Gomes, P. A. J. *Chem. Phys. Lett.* **1998**, *297*, 458.
(27) Russell, J. E.; Shyu, J. S. *J. Chem. Phys.* **1989**, *91*, 1015.
(28) Bratoz, S.; Martin, M. L. *J. Chem. Phys.* **1965**, *42*, 1051.
(29) Hutson, J. M. *BOUND computer code, version 5 (1993)*; distributed by Collaborative Computational Project No. 6 of the Science and Engineering Research Council (UK).
(30) Hutson, J. M. *Comp. Phys. Comm.* **1994**, *84*, *1*.
(31) Hase, W. L. *MERCURY: a general Monte-Carlo classical trajectory computer program*, QCPE 453. An updated version of this code is VENUS96: Hase, W. L.; Duchovic, R. J.; Hu, X.; Komornik, A.; Lim, K. F.; Lu, D.-H.; Peslherbe, G. H.; Swamy, K. N.; van de Linde, S. R.; Varandas, A. J. C.; Wang, H.; Wolf, R. J. *QCPE Bull.* **1996**, *16*, 43.
(32) LeRoy, R. L. *J. Chem. Phys.* **1969**, *73*, 4338.
(33) Roth, P.; Just, T. *Ber. Bunsenges. Phys. Chem.* **1976**, *80*, 171.
(34) Tabayashi, K.; Fueno, T.; Takasa, K.; Kajimoto, O.; Okada, K. *Bull. Chem. Soc. Jpn.* **1977**, *50*, 1754.
(35) Szekely, A.; Hanson, R. K.; Bowman, C. T. *J. Phys. Chem.* **1984**, *88*, 666.
(36) Tsang, W.; Herron, T. *J. Phys. Chem. Ref. Data* **1991**, *20*, 609.
(37) Tsang, W. *J. Phys. Chem. Ref. Data* **1992**, *21*, 753.
(38) Varandas, A. J. C. *Chem. Phys. Lett.* **1994**, *225*, 18.
(39) Marques, J. M. C.; Varandas, A. J. C. *J. Phys. Chem.* **1997**, *101*, 5168.